

Charles University

Faculty of Science

Study programme: Molecular Biology and Biochemistry of Organisms



Shakhkhan Nildikeshev

Structure and function of CAD-ICAD proteins

Struktura a funkce proteinů CAD-ICAD

Bachelor's thesis

Supervisor: RNDr. Josef Novák, Ph.D.

Prague, 2025

Acknowledgements

I would like to express my sincere gratitude to my supervisor Josef Novák for his outstanding support.

Author's Declaration

I, the author of this bachelor's thesis, hereby declare that I have independently prepared this work using the literature listed in the Sources section and with the guidance of my supervisor. In the course of writing, I made use of AI technologies, ScholarGPT and Consensus, to assist with improving the clarity of the text and to support in literature search.

Abstract

Caspase-activated DNase (CAD) and its inhibitor (ICAD) are essential regulators of apoptosis, playing a pivotal role in DNA fragmentation and cellular disintegration. Under proapoptotic conditions, caspase-3 cleaves ICAD within the CAD-ICAD heterodimer, releasing CAD to form homodimers which induce double-strand breaks (DSBs) in nuclear DNA. Beyond apoptosis, the involvement of CAD also has been recognized in cellular differentiation and senescence. In these contexts, ICAD undergoes partial cleavage, allowing for limited CAD activation and controlled DNA damage that contributes to specific cell fate decisions. More recently, CAD-ICAD heterodimers have been shown to serve an additional function in cancer cells. Phosphorylation of specific serine residues on ICAD enables CAD to induce DNA lesions even in its heterodimeric form. These lesions activate DNA damage response that arrest cell cycle progression, giving cancer cells time to repair their genomes. This thesis recapitalizes current knowledge on the functions of CAD and ICAD in apoptosis, differentiation, senescence, and emerging involvement in cell cycle regulation. It also explores the evolutionary origins of the CAD-ICAD system, proposing that its role in DNA damage modulation and cell cycle control may not be limited to malignancy, but could represent a conserved feature across diverse species.

Keywords: Apoptosis, Caspase-activated DNase (CAD), Inhibitor of caspase-activated DNase (ICAD), DNA fragmentation, ICAD phosphorylation.

Abstrakt

Kaspázou aktivovaná DNáza (CAD) a její inhibitor (ICAD) jsou klíčovými regulátory apoptózy, hrajícími zásadní roli ve fragmentaci DNA a rozpadu buňky. V heterodimeru CAD-ICAD dochází při proapoptotických podmínkách ke štěpení ICAD kaspázou 3, čímž se uvolní CAD, který následně vytvoří homodimery s účinnou nukleázovou aktivitou vedoucí k vzniku dvouřetězcových zlomů (DSBs) v jaderné DNA. Mimo apoptózu bylo zapojení CAD pozorováno také při buněčné diferenciaci a senescenci. V těchto případech dochází k částečnému štěpení ICAD, což umožňuje omezenou aktivaci CAD a vznik kontrolovaného poškození DNA, které

přispívá k rozhodnutí o buněčném osudu. Nedávné studie ukázaly, že heterodimery CAD–ICAD mají další funkci v nádorových buňkách. Fosforylace specifických serinových zbytků na ICAD umožňuje CAD indukovat poškození DNA i ve své heterodimerické formě. Tím aktivují odpověď na poškození DNA, která zastavuje buněčný cyklus a dává nádorovým buňkám čas na opravu genomu. Tato práce shrnuje současné poznatky o funkcích CAD a ICAD v apoptóze, diferenciaci, senescenci a jejich nově rozpoznané roli v regulaci buněčného cyklu. Zároveň se zabývá evolučním původem systému CAD–ICAD a navrhuje, že jeho role v modulaci poškození DNA a kontrole buněčného cyklu nemusí být omezena pouze na maligní procesy, ale může představovat konzervovanou vlastnost napříč různými druhy.

Klíčová slova: Apoptóza, Kaspázou aktivovaná DNáza (CAD), Inhibitor kaspázou aktivované DNázy (ICAD), Fragmentace DNA, Fosforylace ICAD.

Contents

1. Introduction	5
2. Apoptotic context of CAD and ICAD	6
3. Structure and expression of CAD and ICAD	8
I. Expression of CAD and ICAD.	8
II. Structure of CAD	9
III. Structure of ICAD	11
IV. CAD-ICAD Heterodimer (DFF Complex)	13
V. CAD- ICAD phosphorylated (CAD-ICADpp)	13
VI. CAD-CAD Homodimer	14
4. Function of CAD and ICAD	16
I. Role of CAD and ICAD in apoptosis	16
II. Roles beyond apoptosis (ICAD cleaved pathway)	17
III. Role in controlling cell cycle (ICAD phosphorylated pathway)	18
5. Evolution of CAD and ICAD	20
6. Conclusion	25
7. Supplementary files:	26
8. Sources	27

1. Introduction

Apoptosis is a well-established mechanism of programmed cell death, with the term "apoptosis" first coined over 50 years ago by (Kerr, Wyllie and Currie, 1972). DNA fragmentation is recognized as one of the hallmarks of apoptosis, with cleavage of chromatin into regular fragments following pro-apoptotic insult first reported in 1976 by a Czechoslovak research team (Skalka, Matyašová and Čejková, 1976). However, the identity of the nuclease responsible for this fragmentation remained unclear for decades. In 1997, Liu and colleagues identified the DNA Fragmentation Factor (DFF), a heterodimeric complex composed of a nuclease, DFF40, and its inhibitor, DFF45 (Liu *et al.*, 1997). Shortly after (Enari *et al.*, 1998), the nuclease and its inhibitor have received their widely accepted names, caspase-activated DNase (CAD) and inhibitor of CAD (ICAD). A detailed structure of CAD was described even later, in 2004 (Woo *et al.*, 2004).

CAD, also known as caspase-activated nuclease (CPAN), DNA fragmentation factor 40 kDa subunit (DFF-40), or DNA fragmentation factor subunit beta (DFFB), is a His-Me finger nuclease (Wu, Lin and Yuan, 2020) that requires Mg^{2+} and Zn^{2+} ions for proper function (Widlak *et al.*, 2000). In its homodimeric (or homo-oligomeric) form, CAD can induce blunt double-strand breaks (DSBs) in linker DNA (Widlak *et al.*, 2000). Under normal conditions, CAD is tightly bound and inhibited by its regulatory partner ICAD, also known as the DNA fragmentation factor 45 kDa subunit (DFF-45) or DNA fragmentation factor subunit alpha (DFFA) (Enari *et al.*, 1998). ICAD exists in two canonical isoforms: shorter ICAD-S and longer ICAD-L.

Both ICAD isoforms can suppress CAD's nuclease activity (Gu *et al.*, 1999). However, only the long isoform (ICAD-L) functions as an effective chaperone, without which CAD cannot properly fold or induce DNA fragmentation (Gu *et al.*, 1999) and only ICAD-L contains nuclear localization signal (NLS) (Samejima and Earnshaw, 2000).

Recent findings have advanced our understanding of CAD and ICAD. This thesis aims to summarize current knowledge of the molecular structure of human CAD and ICAD, explore both classical and modern perspectives on their function, and examine their evolutionary history.

2. Apoptotic context of CAD and ICAD

To fully understand the roles of CAD and ICAD, it is essential to first consider the broader context of apoptotic signaling pathways in which these proteins operate. Apoptosis, a form of programmed cell death, is crucial for eliminating damaged, dysfunctional, or unnecessary cells from the body. It can be initiated through three main pathways — intrinsic (mitochondrial), extrinsic (death receptor-mediated), and perforin/granzyme (cytotoxic T cell-mediated), depending on the type of cellular stress or insult (Elmore, 2007) (**Figure 1**). These pathways converge on a common execution phase, where caspase activation leads to widespread proteolysis and the dismantling of key cellular components, including the activation of the CAD/ICAD system.

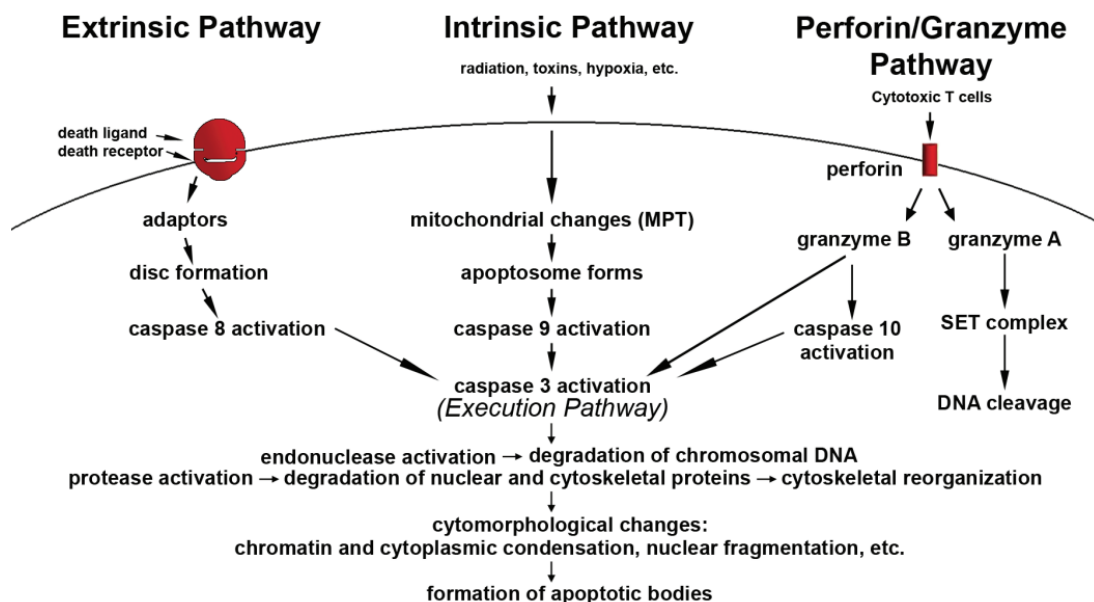


Figure 1. Summary of the apoptotic pathways.

Extrinsic, intrinsic and perforin/granzyme pathways converge in the activation of effector caspases but use different activation cascades to achieve that. Activation of caspase-3 is an irreversible step that starts execution pathway, leading to cell's demise. Adapted from (Elmore, 2007).

In the extrinsic pathway, activation of death receptors on the surface of the cell triggers a signaling cascade that leads to cleavage of procaspase-3 into its active form, caspase-3 (the full pathway is reviewed in (Cavalcante *et al.*, 2019)). Activated caspase-3 then initiates the execution phase of apoptosis by cleaving multiple substrates, including ICAD, thereby releasing active CAD to fragment nuclear DNA (Sakahira, Enari and Nagata, 1998).

Perforin/granzyme pathway may bypass caspase activation entirely, inducing single-stranded DNA breaks through granzyme A in a caspase-independent manner (Beresford *et al.*, 1999). Granzyme B, however, is capable of caspase-3 activation (Darmon, Nicholson and Bleackley, 1995) and therefore can indirectly induce ICAD cleavage.

The intrinsic (mitochondrial) pathway is triggered by internal stressors, such as DNA damage, and involves mitochondrial outer membrane permeabilization (MOMP) (Elmore, 2007). MOMP leads to the release of cytochrome c into the cytosol, where it binds to cofactors to form the apoptosome—a multiprotein complex that activates caspase-3 (Li *et al.*, 1997; Hill *et al.*, 2004).

Caspase-3, also known as CPP32 or apopain, is a cysteine-aspartic endoprotease, which is synthesized as an inactive zymogen (Han *et al.*, 1997), which is called procaspase-3. Each monomer contains an N-terminal prodomain, a large (p20), and a small (p10) catalytic subunit (Steller, 1998). Upon activation, caspase-3 forms a tetramer composed of two p20/p10 heterodimers (Steller, 1998). Each active site cleaves after the last aspartate residue in a sequence of Asp-P2-P3-Asp, with a hydrophobic amino-acid residue at P2 and a hydrophilic amino-acid residue at P3 (EC 3.4.22.56 from ExplorEnz classification list), although the enzyme can accommodate different residues at P2 and P3 (Fang *et al.*, 2006).

As the final step in multiple apoptotic signaling pathways, activated caspase-3 cleaves ICAD, thereby releasing and activating CAD, which then initiates chromatin fragmentation.

3. Structure and expression of CAD and ICAD

I. Expression of CAD and ICAD.

In human, both isoforms of ICAD protein are created by alternative splicing of ICAD pre-mRNA (Kawane *et al.*, 1999), which is encoded by *DFFA* gene, located on the first chromosome on position 1p36.2 (Leek *et al.*, 1997). In both human and mouse, it was shown that ICAD pre-mRNA has 6 exons, and all six of them are present in both ICAD-S and ICAD-L mRNA, but unremoved intron 5 in ICAD-S mRNA leads to earlier stopping of translation and makes the short isoform a product of exons 1-5 (and a short part of expressed intron 5), while the long isoform is a product of all 6 exons (Kawane *et al.*, 1999; Abel *et al.*, 2002). ASF/SF2 protein, a member of highly conserved serine/arginine-rich (SR) protein family, have been shown to play a considerable role in modulating alternative splicing of the ICAD pre-mRNA (Li, Wang and Manley, 2005). Li *et al.* have also shown that depletion of ASF/SF2 protein have switched pre-mRNA splicing pattern to decrease ICAD-L formation but increase ICAD-S isoform formation in chicken DF-40 cell line.

CAD protein is a product of *DFFB* gene, located on the first chromosome on position 1p36.3 (Mukae *et al.*, 1998), relatively close to ICAD's *DFFA* gene. Transcript of the gene has 7 exons, all of which are required for canonical CAD protein (Sugimoto *et al.*, 1999). Nevertheless, aberrant CAD transcripts have been identified in hepatoma cell lines, likely arising from alternative splicing events and splicing errors (Hsieh *et al.*, 2003). Notably, Hsieh *et al.* also report that some of these transcripts feature the replacement of exon 3 with a truncated *Alu* transposable element.

In vitro experiment have shown that ICAD-L protein binds co-translationally with nascent, ribosome bound, CAD polypeptide via Cell Death-Inducing DFF45-like Effector-N (CIDE-N) functional domains, that can be found in both proteins (Sakahira and Nagata, 2002). In this interaction, CIDE-N domain of CAD can fold independently (Otomo *et al.*, 2000), while, at least in *in vitro* conditions, the folding of CIDE-N domain of ICAD-L is induced through its interaction with CAD (Zhou *et al.*, 2001), suggesting that CAD acts as a chaperone for CIDE-N domain of ICAD-L. The folding of CAD's later-translated regions is further assisted by chaperones Hsp70 and Hsp40, in addition to ICAD-L (Sakahira and Nagata, 2002). Interestingly,

one study showed that ICAD-S also retains some chaperone abilities, albeit it is between one and two orders of magnitude less effective at CAD folding (Scholz *et al.*, 2002).

Earlier study (Samejima and Earnshaw, 2000) showed that CAD and ICAD-L are primarily localized in the nucleus, while ICAD-S is mainly cytoplasmic. A more recent study (Sánchez-Osuna *et al.*, 2016), however, showed that in certain glioblastoma cell lines, all three proteins—CAD, ICAD-L, and ICAD-S—can be found in both the cytoplasm and nucleoplasm. Additionally, an experiment demonstrated that nuclear transport of the DFF complex is mediated by the classical importin α/β pathway and requires the NLS regions of both CAD and ICAD-L (Neimanis *et al.*, 2007).

II. Structure of CAD

In humans, CAD consists of 338 amino acids and has a predicted molecular weight of approximately 39.1 kDa (UniProt entry O76075) and pI of 9.3 (Nagata, 2000), its C-terminus contains NLS (Neimanis *et al.*, 2007). CAD consists of three distinct structural domains: CIDE-N (C1), C2, and C3 (**Figure 2A**) (Woo *et al.*, 2004; Kutscher *et al.*, 2012).

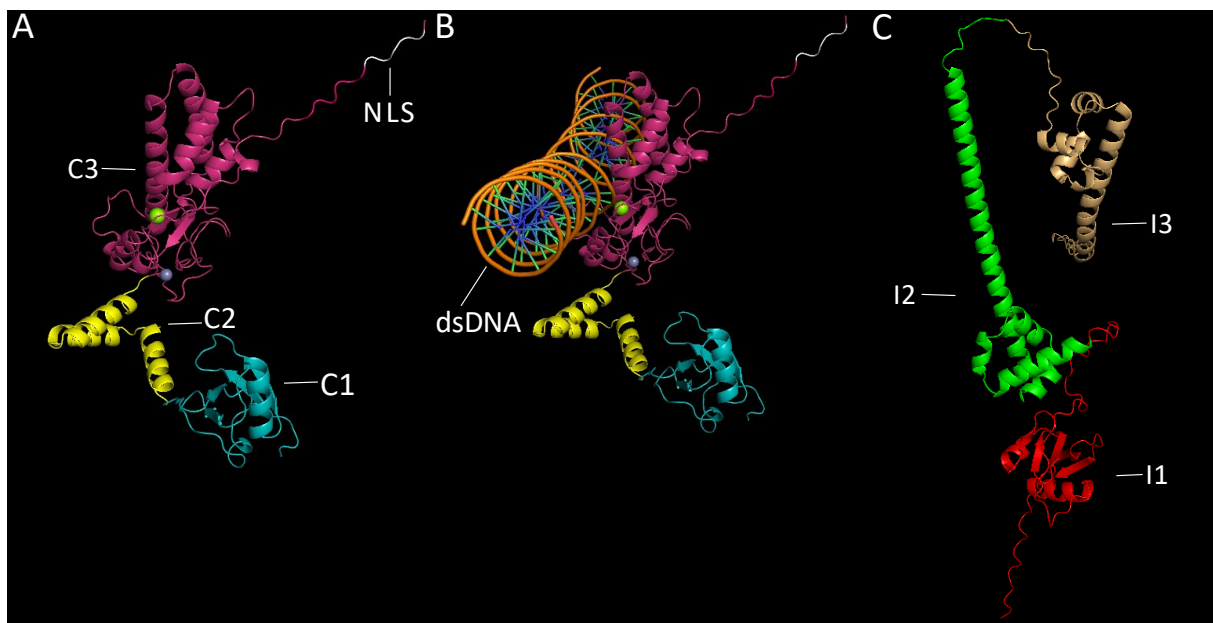


Figure 2: Monomeric structures of human (*Homo sapiens*) CAD, CAD:dsDNA, and ICAD-L.

CAD has three domains: C1 enables CAD-ICAD binding, C2 mediates CAD homodimerization, and C3 provides catalytic activity. Its function depends on Mg^{2+} , while Mn^{2+} stabilizes homodimers. ICAD-L also has three domains: I1 supports CAD binding, I2 disrupts CAD dimerization by targeting C2, and I3 acts as a chaperone essential for proper CAD folding and function. **(A)** Structure of human CAD monomer. Domains are color-coded: cyan for C1 domain, yellow for C2, pink for C3, NLS in the C3 domain is colored white. The green sphere

is Mg^{2+} ion, the grey sphere is Mn^{2+} ion. **(B)** Interaction between dsDNA and CAD monomer, color-coded as above, highlighting CAD's active site placement. The dsDNA chain is in B conformation and consists of normal deoxynucleotides (deoxyadenosine, deoxyguanosine, deoxythymidine, deoxycytidine) in random order, both strands are complementary to each other. It can be seen that Mg^{2+} ion is in the active site. **(C)** Human ICAD-L structure. Domains are color-coded: I1 domain is red, I2 is green, I3 is beige, NLS is not color-coded. All structures are created using AlphaFold3 (Abramson *et al.*, 2024) and visualized by PyMol (The PyMOL Molecular Graphics System, Version 3.0 Schrödinger, LLC.) The structures shown are in the supplement to the thesis.

The CIDE-N domain, also referred to as C1, is located at the N-terminal region of CAD (Inohara *et al.*, 1999). In mouse CAD, this domain spans residues 1–85 and plays a crucial role in binding to ICAD, its inhibitor (Woo *et al.*, 2004). Structurally, it consists of five β -sheets and one α -helix (Otomo *et al.*, 2000). Since this thesis focuses primarily on human CAD and ICAD, and many studies reference their murine orthologs, the author performed a sequence alignment of human and mouse CAD using Clustal Omega (Sievers *et al.*, 2011). This analysis revealed that the C1 domain in human CAD spans residues 1–82. **(Figure 3)**

The C2 domain, found between residues 86–131 in mouse CAD, consists of three α -helices that are essential for CAD homodimerization (Woo *et al.*, 2004). In human CAD this domain corresponds to residues 83–129. **(Figure 3)**

The C3 domain, spanning residues 132–345 in mouse CAD, serves as the catalytic core (Kutscher *et al.*, 2012). This domain contains binding sites for Mg^{2+} and Zn^{2+} ions, both of which play critical roles in CAD activity (Widlak *et al.*, 2000). It was shown that chelating agent ethylenediaminetetraacetic acid (EDTA) is capable of inactivating CAD, showing that Mg^{2+} is essential for CAD's catalytic function (Widlak *et al.*, 2000); Zn^{2+} was shown to be required for stable homodimerization (Woo *et al.*, 2004); however, at high concentrations, Zn^{2+} can also inhibit CAD activity (Widlak *et al.*, 2000).

At the C-terminal region, CAD features an intrinsically disordered segment that includes a nuclear localization signal (NLS), facilitating its transport into the nucleus (Neimanis *et al.*, 2007). In human CAD the C3 domain spans residues 130–338. **(Figure 3)**

```

C1 Domain
sp|054788|DFFB_MOUSE MCAVLRQPKCVKLRALHSACKFGVAARSCQELLRKGCVRFLPMPGSRCLYEDGTEVTD 60
sp|076075|DFFB_HUMAN --MLQKPKSVKLRALRSRKFVAGRSCQEVLRKGCRLRFQLPERGSRLCLYEDGTELTE 57
      *::*:*.*****:* *****.*****:*****:***** *****:*****:*

C2 Domain
sp|054788|DFFB_MOUSE DCFPGLPNDAELELLTAGETWHGYVSDITRFLSVFNPHAGVIQAARQLLSDEQAPLRQK 120
sp|076075|DFFB_HUMAN DYFSPVPDPAELVLLTLGQAWQGYVSDIRRFLSAFHEPQVGLIQAQQLLCDEQAPQRQR 117
      * **.:*::***:*** *::*:***** *****.*:*.:.*:***:***.***** **

C3 Domain
sp|054788|DFFB_MOUSE LLADLLHHVSNITAETREQDPSWFEGLESFRNKSGYLRYSCESRIRGYLREVSAYTSM 180
sp|076075|DFFB_HUMAN LLADLLHNVSQNIAAETRAEDPPWFEGLESRFQSKSGYLRYSCESRIRSYLREVSSYPST 177
      *****:*****:***** :** *****:.....*****:*****:* *

sp|054788|DFFB_MOUSE VDEAAQEEYLRVLGSMCQKLSVQYNGSYFDRGAEASSRLCTPEGWFSCQGPFDLESCLS 240
sp|076075|DFFB_HUMAN VGAEAQEEFLRVLGSMCQLRSMQYNGSYFDRGAKGGSRLCTPEGWFSCQGPFDMSCLS 237
      *. ****:*****:*.*:*****:.....*****:*****:*****

sp|054788|DFFB_MOUSE KHSINPYGNRESRILFSTWNLDHIEKKRTVPTLAEAI--QDGREVNWEYFYSLLFTAE 298
sp|076075|DFFB_HUMAN RHSINPYSNRESRILFSTWNLDHIEKKRTIIPTLVEAIKEQDGREVDWEYFGLLFTSE 297
      :*****.*****:*****:*****:*****:*****:*****:*****:*****

sp|054788|DFFB_MOUSE NLKLVHIACHKKTTHKLECDRSRIYRPQTGSRRKQPARKKRPARKR 344
sp|076075|DFFB_HUMAN NLKLVHIVCHKKTTHKLNCDPSRIYKQTRLKRRKQPVRKRQ----- 338
      *****.*****:*** *****:*** :****.*:*.

```

Figure 3. Alignment of mouse (*Mus musculus*) and human (*Homo sapiens*) CAD proteins

The top line corresponds to murine CAD, the bottom line corresponds to human CAD. The domains of the proteins are color-coded and named. Sequences were obtained from UniProt (<https://www.uniprot.org>), structures O54788 (mouse CAD) and O76075-1 (human canonical isoform of CAD) were used. Alignments were done using Clustal Omega (Sievers *et al.*, 2011) with default parameters. The alignment is in the supplement to the thesis.

III. Structure of ICAD

Inhibitor of CAD exists in two isoforms, ICAD-L (long isoform) and ICAD-S (short isoform), which are generated through alternative splicing (Kawane *et al.*, 1999).

In human, ICAD-S (also known as DFF-35, UniProt entry O00273-2) has 268 amino acids, and predicted molecular weight of ~29.4 kDa, while ICAD-L (also known as DFF-45, UniProt entry O00273-1) has 331 amino acids and predicted molecular weight of ~36.5 kDa. In literature, the term "DFF-45" is sometimes used interchangeably to refer to ICAD in general, but more specifically it often denotes the long isoform, ICAD-L. The molecular weights of DFF-45 and DFF-35 were initially determined by SDS-PAGE/Western blot analysis (Enari *et al.*, 1998; Gu *et al.*, 1999). However, modern annotations, such as those in UniProt, rely on *in silico* predictions using tools like ExPASy ProtParam, which calculates molecular mass based on amino acid sequence (the tool is described in (Walker, 2005)).

ICAD-L consists of three structural domains: the N-terminal domain (I1), the inhibitory domain (I2), and the C-terminal domain (DFF-C) (I3) (**Figure 2C**) ((Kutscher *et al.*, 2012), named D1, D2, D3 by Kutscher *et al.*, here the domains were renamed for better clarity). Alignment of mouse and human ICAD-L isoforms by Clustal Omega (Sievers *et al.*, 2011) shows that ICAD-L has the same length in both humans and mice, with each of its three domains spanning identical residue ranges in both species (**Figure 4**). ICAD have been shown to be resistant to heat (90°C) and denaturant (0.1% SDS) (Enari *et al.*, 1998).

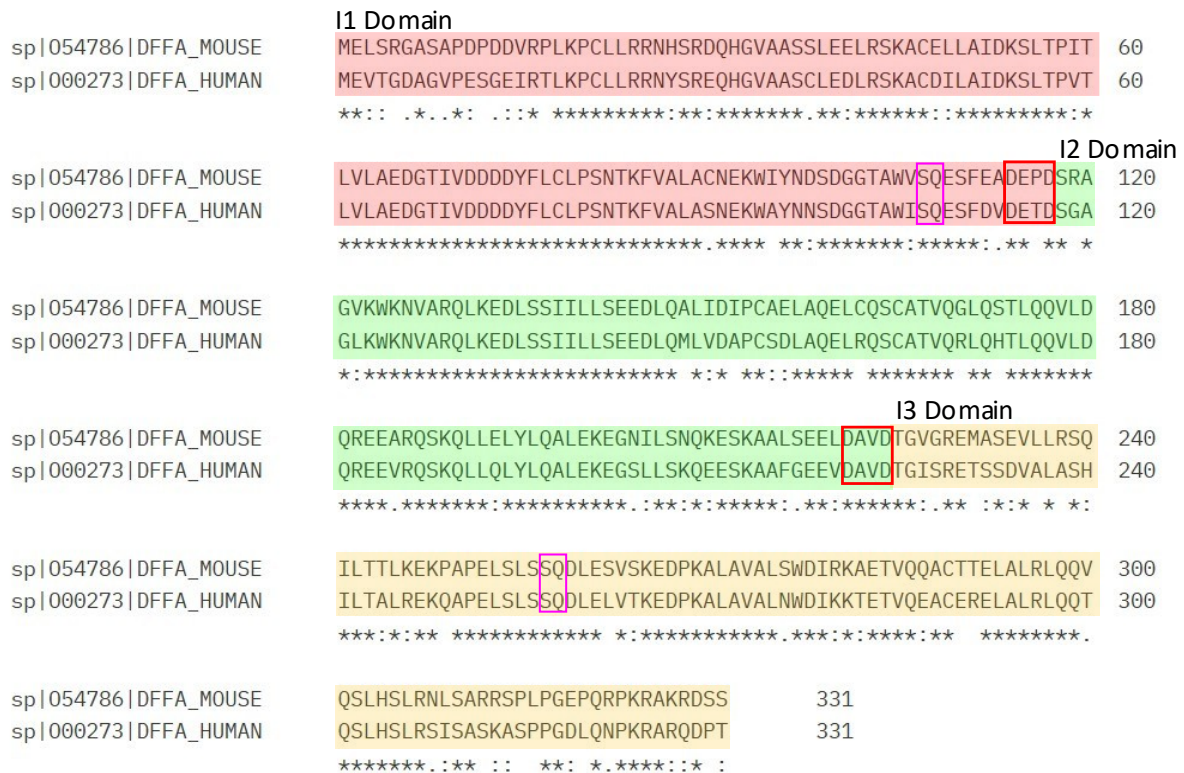


Figure 4. Alignment of mouse (*Mus musculus*) and human (*Homo sapiens*) ICAD-L proteins

The top line corresponds to murine ICAD-L, the bottom line corresponding to human ICAD-L. The domains of the proteins are color-coded and named. Sequences recognized by caspase-3 are highlighted in red, phosphorylation sequences described in (Larsen *et al.*, 2022) highlighted in purple. Sequences were obtained from UniProt, structures O54786-1 (mouse canonical isoform of ICAD-L) and O00273-1 (human canonical isoform of ICAD-L) were used. Alignments were done using Clustal Omega (Sievers *et al.*, 2011) with default parameters. The alignment is in the supplement to the thesis.

The I1 domain, spanning residues 1–117 ((McCarty, Toh and Li, 1999), there D1, D2, and D3 designations were also used), is responsible for a stable interaction of CAD-ICAD, ensuring CAD remains inactive (Kutscher *et al.*, 2012), the N-terminal domain of ICAD includes residues 19-100, which correspond to CIDE-N (Park, 2015). Nuclear magnetic resonance

(NMR) model of interaction between CAD's and ICAD's CIDE-N domains can be observed in (Otomo *et al.*, 2000), corresponding to 1F2R structure in Protein Data Bank (<https://www.rcsb.org/structure/1F2R>). The end of the domain is marked by residue Asp117, necessary for cleaving ICAD by caspase-3 (Sakahira, Enari and Nagata, 1998).

The I2 domain, located between residues 118–224 (McCarty, Toh and Li, 1999), serves as the primary inhibitory region of ICAD. It binds to the C2 domain of CAD, preventing homodimerization, a crucial step for CAD activation. Additionally, this domain partially interacts with the C3 catalytic domain, further suppressing CAD's enzymatic activity (Woo *et al.*, 2004). Residue 224 is aspartic acid, necessary for cleaving ICAD by caspase-3 in the region (Sakahira, Enari and Nagata, 1998).

The I3 domain, spanning residues 225–331 (McCarty, Toh and Li, 1999), is largely absent in ICAD-S and is believed to be essential for ICAD's chaperone function, which ensures the proper folding and stabilization of CAD before activation (Woo *et al.*, 2004).

At the C-terminal region, ICAD-L contains a small, intrinsically disordered segment that includes NLS, necessary for its cellular localization (Samejima and Earnshaw, 2000).

IV. CAD-ICAD Heterodimer (DFF Complex)

In non-apoptotic cells, CAD remains inactive due to its interaction with either isoform of ICAD, forming the CAD-ICAD heterodimer, also known as DFF (DNA Fragmentation Factor) (Gu *et al.*, 1999) (**Figure 5A**). In healthy cells, the CAD-ICAD-L heterodimer is primarily localized in the nucleus, where it remains inactive until apoptotic signals trigger ICAD cleavage (Samejima and Earnshaw, 1998, 2000). However, at least in some glioblastoma cell lines, CAD-ICAD-L can still be found in the cytoplasm at a considerable levels (Sánchez-Osuna *et al.*, 2016).

The ICAD-S isoform, due to its lack of a C-terminal NLS, is primarily confined to the cytoplasm, preventing CAD from entering the nucleus in its inactive state (Samejima and Earnshaw, 2000).

v. CAD- ICAD phosphorylated (CAD-ICADpp)

Recent research suggests that human cancer cells exploit ICAD phosphorylation to regulate DNA damage (Larsen *et al.*, 2022). According to the study, phosphorylation of ICAD-L at serine residues 107 and 257 can allow CAD to make single-strand DNA breaks (SSBs) while

being bound to ICADpp. For visualization purpose, author of this thesis performed computational structure predictions, using AlphaFold3 (Abramson *et al.*, 2024), which show that when ICAD-L is phosphorylated, the I3 domain undergoes a conformational shift, exposing the C3 catalytic domain of CAD (**Figure 5B**). This structural rearrangement may play a crucial role in initiating DNA damage and promoting genomic stability in cancer cells.

VI. CAD-CAD Homodimer

After ICAD cleavage by caspase-3, CAD becomes active and forms homodimers, adopting a structure resembling molecular scissors, as determined experimentally (Woo *et al.*, 2004), visualization of human structure made by AlphaFold3 can be seen in **Figure 5C**. These homodimers function as endonucleases, capable of cutting linker DNA and generating blunt double-strand breaks (DSBs) or 1-base 5'-overhangs with 5'-phosphate and 3'-hydroxyl groups (Widlak *et al.*, 2000). Studies show that the dimer may create DSBs by cleaving each DNA strand stepwise in special *in vitro* conditions (Widlak and Garrard, 2001) and potentially in *in cellula* conditions as well (Iglesias-Guimaraes *et al.*, 2013). Although CAD does not exhibit strong DNA sequence specificity, it shows a tendency to cleave AT-rich regions more frequently (Widlak *et al.*, 2000). Interestingly, CIDE-N domains are reported to interact in head-to-tail fashion to form higher-order, spiral-like CAD homo-oligomers (Choi *et al.*, 2017).

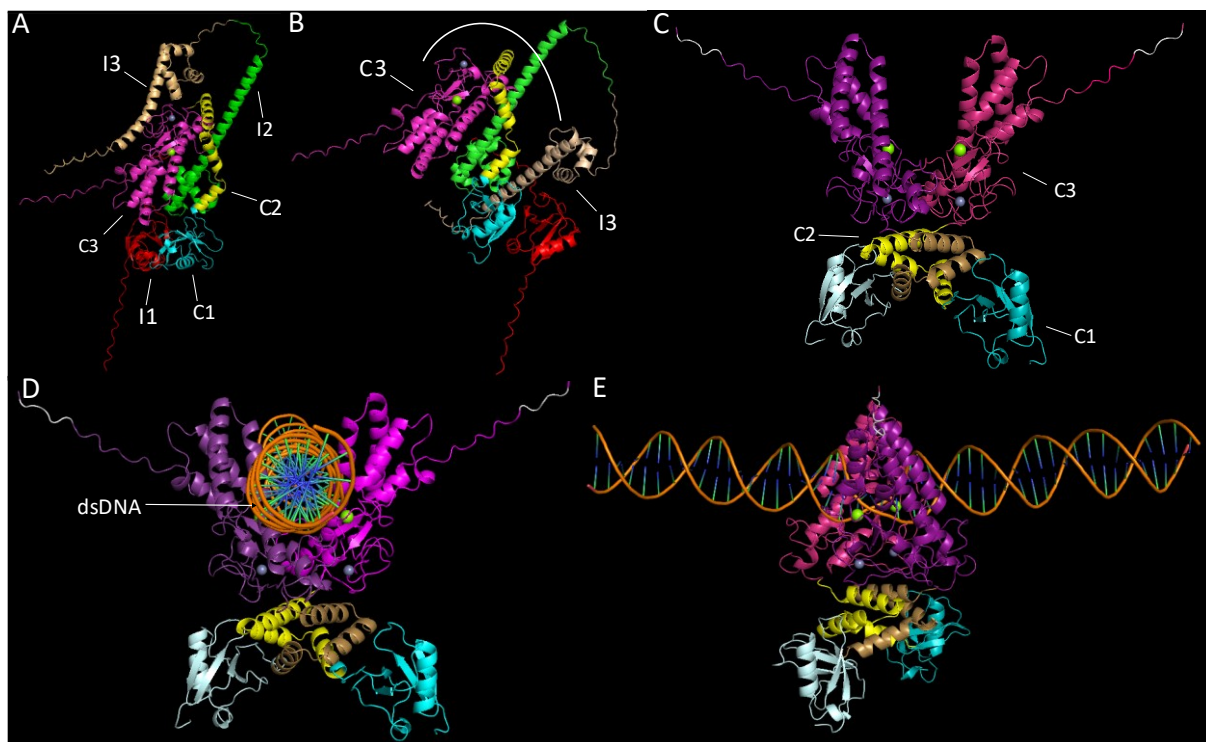


Figure 5: Dimeric structures of human (*Homo sapiens*) CAD-ICAD-L, CAD-ICAD-L phosphorylated (CAD-ICADpp), CAD-CAD, CAD-CAD:dsDNA.

(A) Human CAD-ICAD-L heterodimer. Each domain and ions are color-coded as in Figure 2, NLS are not colored. I1 and C1 domains interact, C2 domain is disassembled by interactions with I2, C3 domain still binds both Mg^{2+} and Mn^{2+} ions, and is tilted in comparison with free CAD's C3 domain, I3 domain covers active site and ions of C3. **(B)** CAD-ICADpp heterodimer. In comparison with unphosphorylated structure from Figure 4A, the phosphorylation of ICAD-L on S107 and S257 changes position of I3 domain, uncovering C3 domain's active site and ions bound to CAD. **(C)** CAD-CAD homodimer. The homodimer creates a scissor-like structure. The same domains of different monomers have similar colors of different gamma, NLS in both domains are white. The green spheres are Mg^{2+} ion, the grey spheres are Mn^{2+} ion. Annotations on the picture show the domains of the same monomer. **(D)** Interactions between CAD-CAD homodimer and dsDNA, highlighting active site of the "scissors". Color coding is the same as in Figure 5C. The dsDNA chain is in B conformation and consists of normal deoxynucleotides (deoxyadenosine, deoxyguanosine, deoxythymidine, deoxycytidine) in random order, both strands are complementary to each other. Interestingly, the direct interaction between CAD-CAD and dsDNA was predicted at AT rich sequence. **(E)** Side view of CAD-CAD homodimer interactions with dsDNA. Both CAD-CAD and DNA are identical to those described in Figure 5D. All structures are created using AlphaFold3 (Abramson et al., 2024) and visualized by PyMol (The PyMOL Molecular Graphics System, Version 3.0 Schrödinger, LLC.) The structures shown are in the supplement to the thesis.

4. Function of CAD and ICAD

I. Role of CAD and ICAD in apoptosis

Although ICAD can be cleaved by caspases -3 and -7 (Wolf *et al.*, 1999), caspase-3 is considered the most efficient and physiologically relevant enzyme for CAD activation via ICAD cleavage. In humans, both ICAD isoforms are cleaved after the final aspartic acid residues in the motifs DEPD (position 117) and DAVD (position 224), resulting in ICAD inactivation and subsequent release of CAD from inhibition (Sakahira, Enari and Nagata, 1998). Importantly, cleavage at D117 plays a more critical role in CAD activation (Yuste *et al.*, 2005), since cells unable to cleave ICAD at this site do not exhibit DNA fragmentation, whereas those lacking cleavage at D224 still undergo normal apoptosis. Following ICAD cleavage, CAD homodimerizes and cleaves chromosomal DNA into nucleosomal fragments, generating the characteristic DNA laddering pattern observed during apoptosis (Sakahira, Enari and Nagata, 1998). However, under *in vivo* conditions, CAD may not be sufficient to accomplish complete internucleosomal DNA fragmentation on its own. In certain cancer cell lines, it has been shown to cooperate with DNAS1L3 (also known as DNase γ), a Ca^{2+} -dependent endonuclease, to fully degrade chromatin DNA into nucleosomal units (Errami *et al.*, 2013).

More broadly, CAD plays an essential role in the structural disassembly of the nucleus during apoptosis. While early nuclear changes, such as chromatin condensation, can occur independently of CAD, later-stage events like nuclear fragmentation and collapse depend on CAD's activity (Iglesias-Guimaraes *et al.*, 2013). Specifically, CAD is required to generate single-strand DNA breaks (SSBs) with free 3'-OH ends, which are critical for nuclear disintegration (Iglesias-Guimaraes *et al.*, 2013). Notably, Iglesias-Guimaraes *et al.* showed that CAD is responsible for most SSBs observed in the apoptotic nucleus.

Although DNA fragmentation by CAD is a hallmark of apoptosis, it is not strictly essential for cell death to occur. Mice lacking functional CAD due to ICAD-L deficiency exhibit no DNA laddering in immune cells yet show normal immune system development (Zhang *et al.*, 1998), despite the known role of apoptosis in this process (most directly reviewed in (Opferman, 2008)). Nonetheless, DNA degradation is considered a key step in marking the cell for clearance. It has been shown that degraded DNA acts as a chemoattractant, critical for efficient phagocytosis of apoptotic cell remains (Elliott *et al.*, 2009), and it was hypothesized

that unfragmented, “naked” DNA could be dangerous to neighboring cells by “potentially integrating and disrupting their genomes” (Wyllie, 1998).

II. Roles beyond apoptosis (ICAD cleaved pathway)

While CAD is best known for its role in apoptosis, subapoptotic activation of caspase-3 and CAD also plays a critical role in influencing cell fate decisions, particularly in differentiation. For instance, in skeletal muscle differentiation, transient activation of caspase-3 leads to partial cleavage of ICAD at D117 (cleavage at D224 was not reported), leading to limited activation of CAD and the generation of SSBs in DNA at specific loci (Larsen *et al.*, 2010). These DNA lesions are not destructive but rather serve as critical signaling events that initiate myoblast differentiation. Notably, CAD-mediated damage within the promoter region of p21, a key regulator of cell cycle arrest, appears to upregulate its expression, thereby promoting the terminal differentiation of muscle cells.

Further supporting this model, later study (Al-Khalaf *et al.*, 2016) reinforced the theory by finding that in the process of muscle differentiation presence of repair protein XRCC1—essential for base excision repair (BER), which resolves SSBs—is crucial for muscle differentiation. Moreover, Al-Khalaf *et al.* found that the expression of p21 is dependent on XRCC1 activity reinforcing the idea that CAD-induced DNA damage and subsequent repair are functionally linked to the transcriptional regulation in muscle cells.

The importance of caspase-3 in cellular differentiation extends beyond muscle tissue. In various mammalian lineages—including lens fiber epithelial cells, keratinocytes, erythrocytes and bone marrow cells—differentiation is impaired when caspase-3 activity is inhibited (Ishizaki, Jacobson and Raff, 1998; Weil, Raff and Braga, 1999; Zermati *et al.*, 2001; Miura *et al.*, 2004). Since ICAD is a principal substrate of caspase-3, it is plausible that CAD contributes to these differentiation processes by mediating downstream DNA modifications. The conservation of caspase-dependent differentiation pathways across diverse metazoans supports the hypothesis that CAD functions extend beyond apoptosis, potentially representing an evolutionarily conserved mechanism of cell fate regulation (hypothesis proposed in (Bell and Megeney, 2017)).

In addition to differentiation, CAD also appears to be involved in cellular senescence. A recent study demonstrated that sublethal activation of CAD induces senescence in both

murine and human non-cancerous cells (Haimovici *et al.*, 2024). In this study, CAD-deficient cells exhibited significantly reduced senescence markers, including diminished cell cycle arrest, lower expression of senescence-associated genes, and decreased IL-6 secretion. The study further showed that direct activation of CAD via ICAD degradation was sufficient to induce a full senescence-associated phenotype. Notably, in mouse embryonic fibroblasts and human keratinocyte HaCaT cells, CAD activation led to upregulation of *p21*, a key mediator of the senescence response.

Other findings also imply that CAD plays a role in inducing senescence of human tumor cells. In various cancer cell lines treated with MOMP-inducing agent, cells that resist apoptosis undergo p53-dependent senescence (Song *et al.*, 2011). This response is triggered by partial MOMP, resulting in low-level cytochrome c release and sublethal caspase-3 activation. As a result, ICAD is cleaved, CAD becomes partially active, and introduces DNA lesions, which are marked by γ H2AX phosphorylation and activate p53, ultimately leading to a permanent growth arrest.

Conversely, in untreated cancers, CAD activity may support malignant progression. One study (Haimovici *et al.*, 2022) demonstrated that minor MOMP can activate CAD, leading to the formation of micronuclei, which are linked to invasive growth and chromosomal instability. Transcriptomic analysis of CAD-deficient HeLa and MDA-MB231 cells revealed altered expression of genes associated with epithelial-mesenchymal transition (EMT) and cellular invasiveness. The findings suggest that CAD-associated gene expression patterns may be linked to poor clinical outcomes. Interestingly, CAD-deficient tumor cells did not show impaired viability compared to their wild-type counterparts, indicating that CAD may serve more as a pro-tumorigenic modulator of the tumor environment rather than a simple executioner of apoptosis.

III. Role in controlling cell cycle (ICAD phosphorylated pathway)

According to a recent article (Larsen *et al.*, 2022), activation of CAD's catalytic function does not require cleavage of ICAD-L. Following exposure to ionizing radiation, and subsequent DNA damage, cancer cells use DNA damage response mechanisms to phosphorylate ICAD-L at S107 and S257, leaving CAD attached to ICAD-L, but allowing CAD to act as a source of DNA damage, predominantly in form of SSBs, but not allowing it to homodimerize. This mechanism

involves ATM (ataxia telangiectasia mutated) and ATR (ataxia telangiectasia and RAD3-related) kinases that phosphorylate ICAD-L, and PARP-1 (poly(ADP-ribose)polymerase-1) for repair of lesions, caused by CAD. The irradiated cells use this pathway to make a second wave of DNA lesions ~24 hours after exposure to ionizing radiation (the first wave is induced by the irradiation), allowing the tumor cells to stall progression of cell cycle by activating G2 checkpoint. Postponed cell cycle progression gives time to cancer cells for finishing DNA repairs, improving genome stability and cell survival. It is not clear, however, how the cancer cells time the second wave of DNA damage, since ATM/ATR-mediated response takes place rapidly after irradiation (Hartlerode *et al.*, 2015), so there is most likely another mechanism of delay of second wave DNA damage. Interestingly, this pathway does not involve caspase-3 activation, as neither ICAD cleavage nor caspase-3 activity in general were detected, and pan-caspase inhibition did not affect induction of new DNA breaks ~24 hours after irradiation.

Currently this is the only known instance of CAD activation via ICAD's post-translational modification, however high throughput phosphoproteomic datasets, in particular PhosphoSitePlus (Hornbeck *et al.*, 2015), show other instances of phosphorylation on ICAD, most notably Y75 and S315 have been shown carrying phosphate group in 32 and 34 mass spectroscopy references, respectively, at the time of writing. For comparison, S107 and S257 have 11 and 8 references, respectively, at the time of writing. These references, however, do not discuss functions of phosphorylations on ICAD, but many of them are related to cancer research, further hinting at possible post-translational regulation of ICAD in tumors. Specifically, 2 studies (Curated info on PhosphoSitePlus, referencing (Chen *et al.*, 2009; Hsu *et al.*, 2011)) found links between mTOR, a key regulator of cell cycle, and its inhibitor rapamycin with ICAD's phosphorylation on S110 and S315. Additionally, Y75 have been shown to have a significant role in CAD-ICAD interactions (Otomo *et al.*, 2000).

5. Evolution of CAD and ICAD

The CAD and ICAD proteins, encoded by the *DFFB* and *DFFA* genes respectively, appear to have originated early in animal evolution. These proteins are conserved across a wide range of species, including members of evolutionarily ancient clades (Wu *et al.*, 2008). In Cnidarians, both CAD and ICAD have been identified in species such as *Nematostella vectensis* (starlet sea anemone) (Eckhart, Fischer and Tschachler, 2007) and *Hydra vulgaris* (hydra, a fresh-water polyp) (Wu *et al.*, 2008), have both ICAD and CAD. In Porifera, the sponge *Geodia cydonium* exhibits caspase-3-dependent apoptosis with DNA fragmentation (Wiens *et al.*, 2003), however, BLAST searches (Altschul *et al.*, 1990), performed by the thesis's author using the human CAD sequence did not reveal clear homologs in this species. Interestingly, BLAST search in Porifera revealed structures closely resembling CAD (accession number XP_065183936.1) (Figure 6) and ICAD (accession number XP_065183937.1) in *Sycon ciliatum*. These findings suggest that both CAD and ICAD were already present in the last common ancestor of the Metazoa clade.

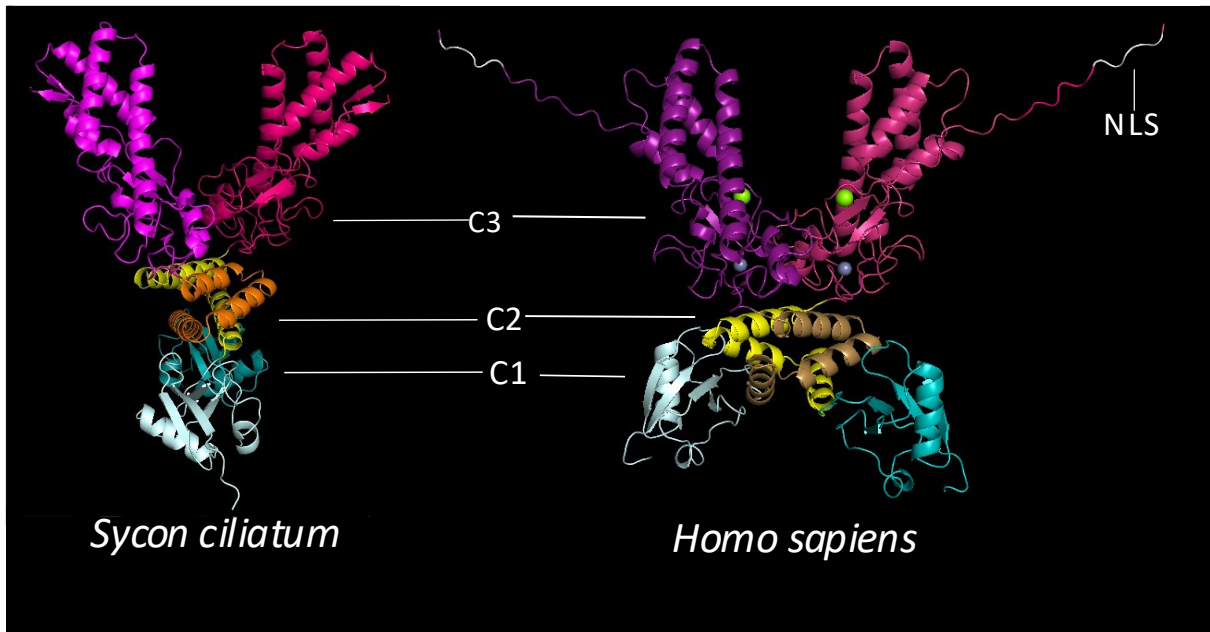


Figure 6. Comparison of CAD-CAD dimers in *Sycon ciliatum* and human.

Both dimers have characteristic scissors-like structure, with C1 and C2 of *S. ciliatum* twisted by $\sim 90^\circ$ in comparison to those of human. The same domains of different monomers have similar colors of different gamma. NLS, Mg^{2+} (green sphere) and Mn^{2+} (grey sphere) ions are shown only in human CAD-CAD dimer. All structures are created using AlphaFold3 (Abramson *et al.*, 2024) and visualized by PyMol (The PyMOL Molecular Graphics System, Version 3.0 Schrödinger, LLC.) The structures shown are in the supplement to the thesis.

Strikingly, the evolutionary history of CAD and ICAD may extend beyond the Metazoa clade. At the time of writing, BLAST searches using the human CAD sequence across non-metazoan organisms return no clear homologs of non-synthetic origin. However, a recent study identified a CAD ortholog in *Giardia lamblia* (Villa-Medina *et al.*, 2025), a flagellated parasitic protozoan microorganism that does not possess functional mitochondria (Bagchi *et al.*, 2012). Villa-Medina *et al.* also reported that the *G. lamblia* CAD ortholog contains a CIDE-N domain—an essential motif for proper folding and activation by ICAD—suggesting that this protozoan may also possess an ICAD-like protein, although further confirmation is required (author’s BLAST searches did not identify a clear ICAD homolog). Interestingly, *Giardia* has been shown to undergo apoptosis-like programmed cell death characterized by DNA fragmentation under oxidative stress, despite absence of caspase genes in its genome and detectable caspase-like activity. One possible explanation for the presence of CAD in *G. lamblia* may be horizontal gene transfer from another species. However, sequence analysis reveals only 22.43% identity between the *Giardia* CAD and human CAD (Villa-Medina *et al.*, 2025). Moreover, multiple sequence alignment done by the thesis’s author, comparing CAD from *Giardia lamblia*, *Sycon ciliatum* (sponge), *Nematostella vectensis* (sea anemone), and *Hydra vulgaris* (hydra) show minimal sequence similarity (**Figure 7**), reinforcing the notion that the *G. lamblia* CAD is evolutionarily distant from even the most ancient metazoan counterparts. These findings hint at either an ancient and highly divergent origin of the CAD gene or an independent evolutionary pathway in this protozoan lineage.

is not exclusive to CAD and ICAD; it is also found in a group of related proteins—CIDE-A, CIDE-B, and CIDE-C—which are unique to vertebrates and are involved in lipid metabolism and energy homeostasis (Inohara *et al.*, 1998; Liang *et al.*, 2003). According to (Wu *et al.*, 2008), CIDE-N domains of CIDE proteins are most closely related to that of ICAD and the presence of CIDE proteins exclusively in vertebrates supports the 2R whole-genome duplication hypothesis. In line with the 2R hypothesis, it is proposed that the CIDE gene family first emerged from an ancestral ICAD gene during an early vertebrate genome duplication event, with a subsequent duplication giving rise to distinct CIDE proteins in both Agnatha (jawless vertebrates) and Gnathostomata (jawed vertebrates). This highlights ICAD's pivotal role as a genomic precursor within the expanded CIDE protein family.

Interestingly, CAD and ICAD may have served as evolutionary templates for the development of a broader range of proteins. Domain architecture search of the thesis's author using InterPro (<https://www.ebi.ac.uk/interpro>), focused on the characteristic combination of a CIDE-N domain and an effector domain of CAD or ICAD, revealed a surprising diversity of protein configurations across taxa. Among these are proteins containing only a functional domain, as well as proteins combining CIDE-N with entirely different domains. For example, a protein with accession number A0A1J7IBC6 belongs to a fungus of Ascomycota clade and has DFF-C as well as other domains involved in processing of sugars.

An analysis of specific phosphorylation sites in ICAD, described in (Larsen *et al.*, 2022) reveals intriguing patterns of evolutionary conservation that may reflect functional significance. The mentioned study identified and demonstrated the role of two conserved phosphorylation sites in ICAD of mammals, corresponding to human's S107 and S257. The author of the thesis extended this bioinformatic investigation across 32 species. Multiple sequence alignment of ICAD proteins shows (**Figure 8**) that the phosphorylation site corresponding to human S107 is well conserved across examined mammals. In these species, the residue consistently appears as an SQ motif, a well-established target for phosphorylation by ATM/ATR kinases (Traven and Heierhorst, 2005). In birds, reptiles, and legless amphibians, a serine residue is present at the analogous position, but the critical glutamine that follows in the canonical SQ motif is absent, suggesting potential divergence in kinase recognition or regulation. The second phosphorylation site, corresponding to human S257, shows even broader conservation. The SQ motif is preserved not only in mammals, but also in birds,

reptiles, and at least one species of legless amphibian. This widespread conservation suggests a conserved regulatory mechanism involving CAD-ICAD phosphorylation across Tetrapoda and supports the idea that these sites are functionally significant rather than retained by chance.

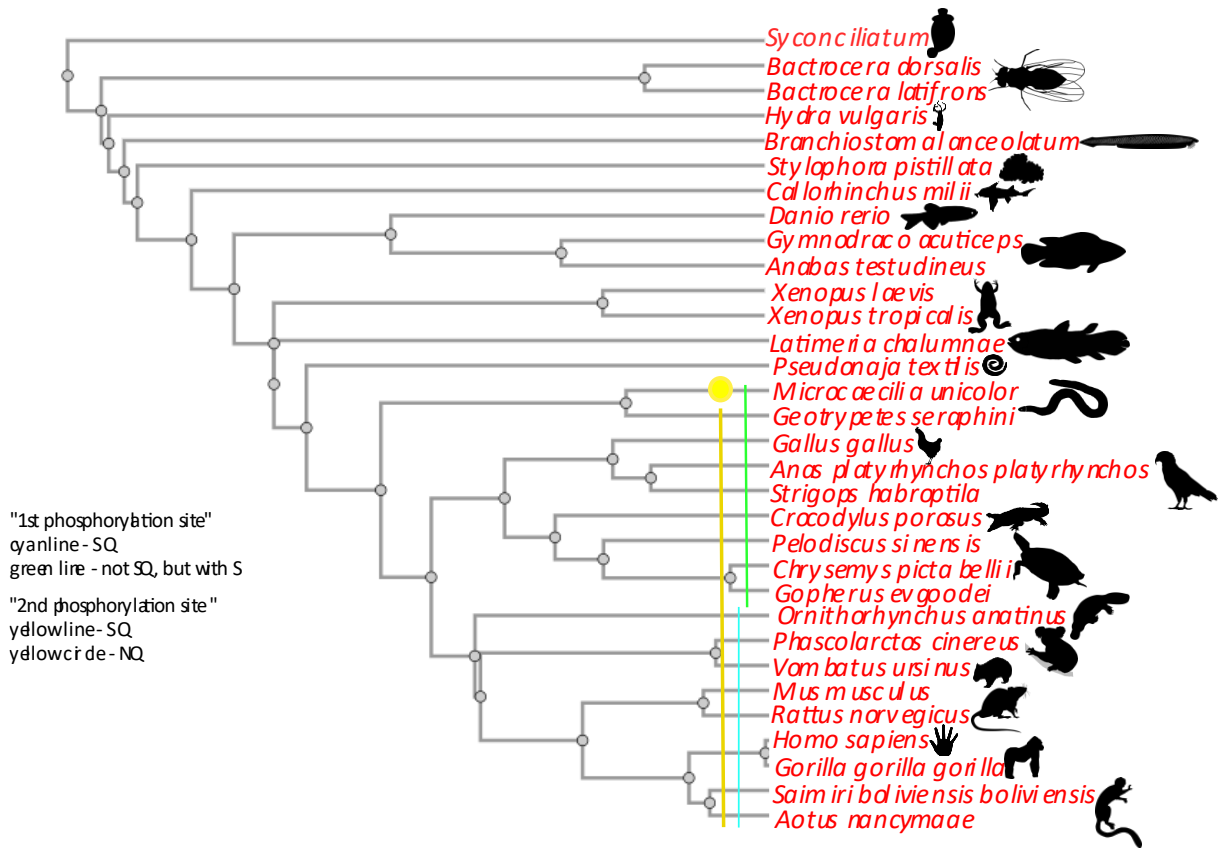


Figure 8. Phylogenetic tree of ICAD in select species

Despite the unusual placement of certain ICAD proteins, the tree shows that specific phosphorylation sites are preserved in many species. “1st phosphorylation site” corresponds to human’s S107, “2nd phosphorylation site” corresponds to human’s S257. Silhouettes of the animals were obtained from PhyloPic (<https://www.phylopic.org>) and can correspond to more than 1 specie. The species were selected in a way that a taxon would have 3 representatives, where possible. If a specie had more than 1 ICAD isoform, the longest one was chosen. Sequences were obtained from BLAST searches and from UniProt. Accession numbers of the sequences as well as alignments used are in the supplement to the thesis. Alignments were done using Custal Omega (Sievers *et al.*, 2011) with default parameters.

Additionally, the residue corresponding to human ICAD’s Y75—a key site implicated in CAD-ICAD interaction—is extremely well conserved across all studied species, with only *Branchiostoma lanceolatum* (a lancelet) substituting a phenylalanine, a chemically similar aromatic residue. This highlights the critical role of Y75 in maintaining CAD-ICAD structural integrity. In contrast, the residue corresponding to S315 appears to be conserved exclusively within primates.

6. Conclusion

CAD and ICAD are well-established components of the apoptotic pathways, responsible for fragmenting chromatin (Woo *et al.*, 2004). However, a growing body of evidence shows that the functional scope of CAD and ICAD extends beyond classical apoptosis. Sublethal activation of apoptotic pathways can result in limited cleavage of ICAD and partial activation of CAD, triggering non-lethal cellular responses. These include cellular senescence (Haimovici *et al.*, 2024), sometimes used for tumor-suppressive consequences (Song *et al.*, 2011), as well as terminal differentiation in several cell lineages, such as myoblasts (Larsen *et al.*, 2010).

Intriguingly, some of these alternative functions may be co-opted by tumor cells. While cancer cells are known to exploit subapoptotic signaling for their advantages (Haimovici *et al.*, 2022), a study (Larsen *et al.*, 2022) has revealed a novel mechanism in which malignant utilize CAD activity to stall the cell cycle and provide time for DNA repair. The conservation of these phosphorylation sites across mammalian species, mentioned in Larsen *et al.* 2022, suggests that this mechanism is not unique to cancer but likely serves a physiological role in normal cells.

To explore this further, this thesis includes a multiple sequence alignment of ICAD across multiple species. The analysis reveals that the key phosphorylation sites in ICAD can be found in many Tetrapoda species, supporting the hypothesis that phosphorylation-mediated regulation of ICAD is an evolutionary conserved mechanism, potentially linked to DNA damage response pathways. This regulatory axis may be exploited by cancer cells to maintain genomic integrity under stress, as discussed in Larsen *et al.*, 2022.

Despite decades of research, several questions about CAD and ICAD remain unresolved. Their evolutionary origin is still by the most part unclear, as homologs of these proteins are present not only in early metazoans but also in some unicellular eukaryotes. In particular, CAD-like sequences found in protists such as *Giardia lamblia* (Villa-Medina *et al.*, 2025) appear to be evolutionarily distinct. Additionally, domains resembling those of CAD and ICAD have been identified in non-metazoan lineages, including members of the Ascomycota phylum (like an InterPro entry with accession number A0A1J7IBC6), suggesting a deeper and more complex evolutionary history.

Understanding the multifaceted roles of CAD and ICAD can enhance our knowledge of not only apoptotic mechanisms but also tumor suppression and broader evolutionary trends in eukaryotic biology.

7. Supplementary files:

- Alignments
 - Alignment_CAD_mouse_vs_human – alignment from Figure 3
 - Alignment_ICAD_mouse_vs_human - alignment from Figure 4
 - Alignment_parasite_vs_metazoa – alignment from Figure 7
 - Alignment_phylogenetic_tree - alignment from Figure 8
 - names_of_sequences_for_the_tree – list of accession numbers used for phylogenetic tree in Figure 8
 - sequences_of_32_species – list of sequences used for phylogenetic tree in Figure 8
- Structures (used for both mono- and dimers)
 - CAD_CAD_dsDNA_ions – structure of CAD-CAD homodimer with dsDNA
 - CAD_CAD_sponge - structure of CAD-CAD homodimer of *Sycon ciliatum*
 - CAD_ICAD_colored_ions - structure of CAD-ICAD-L
 - CAD_ICADpp_ions - structure of CAD-ICAD-L phosphorylated

8. Sources

- Abel, F. *et al.* (2002) 'Analyses of apoptotic regulators CASP9 and DFFA at 1P36.2, reveal rare allele variants in human neuroblastoma tumours', *British Journal of Cancer*, 86(4), pp. 596–604. Available at: <https://doi.org/10.1038/sj.bjc.6600111>.
- Abramson, J. *et al.* (2024) 'Accurate structure prediction of biomolecular interactions with AlphaFold 3', *Nature*, 630(8016), pp. 493–500. Available at: <https://doi.org/10.1038/s41586-024-07487-w>.
- Al-Khalaf, M.H. *et al.* (2016) 'Temporal activation of XRCC1-mediated DNA repair is essential for muscle differentiation', *Cell Discovery*, 2(1), pp. 1–13. Available at: <https://doi.org/10.1038/celldisc.2015.41>.
- Altschul, S.F. *et al.* (1990) 'Basic local alignment search tool', *Journal of Molecular Biology*, 215(3), pp. 403–410. Available at: [https://doi.org/10.1016/S0022-2836\(05\)80360-2](https://doi.org/10.1016/S0022-2836(05)80360-2).
- Bagchi, S. *et al.* (2012) 'Programmed cell death in Giardia', *Parasitology*, 139(7), pp. 894–903. Available at: <https://doi.org/10.1017/S003118201200011X>.
- Bell, R.A.V. and Megeney, L.A. (2017) 'Evolution of caspase-mediated cell death and differentiation: twins separated at birth', *Cell Death & Differentiation*, 24(8), pp. 1359–1368. Available at: <https://doi.org/10.1038/cdd.2017.37>.
- Beresford, P.J. *et al.* (1999) 'Granzyme A Loading Induces Rapid Cytolysis and a Novel Form of DNA Damage Independently of Caspase Activation', *Immunity*, 10(5), pp. 585–595. Available at: [https://doi.org/10.1016/S1074-7613\(00\)80058-8](https://doi.org/10.1016/S1074-7613(00)80058-8).
- Cavalcante, G.C. *et al.* (2019) 'A Cell's Fate: An Overview of the Molecular Biology and Genetics of Apoptosis', *International Journal of Molecular Sciences*, 20(17), p. 4133. Available at: <https://doi.org/10.3390/ijms20174133>.
- Chen, R.-Q. *et al.* (2009) 'CDC25B mediates rapamycin-induced oncogenic responses in cancer cells', *Cancer Research*, 69(6), pp. 2663–2668. Available at: <https://doi.org/10.1158/0008-5472.CAN-08-3222>.
- Choi, J.Y. *et al.* (2017) 'CIDE domains form functionally important higher-order assemblies for DNA fragmentation', *Proceedings of the National Academy of Sciences*, 114(28), pp. 7361–7366. Available at: <https://doi.org/10.1073/pnas.1705949114>.
- Darmon, A.J., Nicholson, D.W. and Bleackley, R.C. (1995) 'Activation of the apoptotic protease CPP32 by cytotoxic T-cell-derived granzyme B', *Nature*, 377(6548), pp. 446–448. Available at: <https://doi.org/10.1038/377446a0>.
- Eckhart, L., Fischer, H. and Tschachler, E. (2007) 'Phylogenomics of caspase-activated DNA fragmentation factor', *Biochemical and Biophysical Research Communications*, 356(1), pp. 293–299. Available at: <https://doi.org/10.1016/j.bbrc.2007.02.122>.
- Elliott, M.R. *et al.* (2009) 'Nucleotides released by apoptotic cells act as a find-me signal to promote phagocytic clearance', *Nature*, 461(7261), pp. 282–286. Available at: <https://doi.org/10.1038/nature08296>.

Elmore, S. (2007) 'Apoptosis: A Review of Programmed Cell Death', *Toxicologic Pathology*, 35(4), pp. 495–516. Available at: <https://doi.org/10.1080/01926230701320337>.

Enari, M. *et al.* (1998) 'A caspase-activated DNase that degrades DNA during apoptosis, and its inhibitor ICAD', *Nature*, 391(6662), pp. 43–50. Available at: <https://doi.org/10.1038/34112>.

Errami, Y. *et al.* (2013) 'Apoptotic DNA Fragmentation May Be a Cooperative Activity between Caspase-activated Deoxyribonuclease and the Poly(ADP-ribose) Polymerase-regulated DNAS1L3, an Endoplasmic Reticulum-localized Endonuclease That Translocates to the Nucleus during Apoptosis*', *Journal of Biological Chemistry*, 288(5), pp. 3460–3468. Available at: <https://doi.org/10.1074/jbc.M112.423061>.

Fang, B. *et al.* (2006) 'Structural and Kinetic Analysis of Caspase-3 Reveals Role for S5 Binding Site in Substrate Recognition', *Journal of Molecular Biology*, 360(3), pp. 654–666. Available at: <https://doi.org/10.1016/j.jmb.2006.05.041>.

Gu, J. *et al.* (1999) 'Functional Interaction of DFF35 and DFF45 with Caspase-activated DNA Fragmentation Nuclease DFF40*', *Journal of Biological Chemistry*, 274(30), pp. 20759–20762. Available at: <https://doi.org/10.1074/jbc.274.30.20759>.

Haimovici, A. *et al.* (2022) 'Spontaneous activity of the mitochondrial apoptosis pathway drives chromosomal defects, the appearance of micronuclei and cancer metastasis through the Caspase-Activated DNase', *Cell Death & Disease*, 13(4), pp. 1–14. Available at: <https://doi.org/10.1038/s41419-022-04768-y>.

Haimovici, A. *et al.* (2024) 'The caspase-activated DNase promotes cellular senescence', *The EMBO Journal*, 43(16), pp. 3523–3544. Available at: <https://doi.org/10.1038/s44318-024-00163-9>.

Han, Z. *et al.* (1997) 'A Sequential Two-Step Mechanism for the Production of the Mature p17:p12 Form of Caspase-3 *in Vitro* *', *Journal of Biological Chemistry*, 272(20), pp. 13432–13436. Available at: <https://doi.org/10.1074/jbc.272.20.13432>.

Hartlerode, A.J. *et al.* (2015) 'Recruitment and activation of the ATM kinase in the absence of DNA-damage sensors', *Nature Structural & Molecular Biology*, 22(9), pp. 736–743. Available at: <https://doi.org/10.1038/nsmb.3072>.

Hill, M.M. *et al.* (2004) 'Analysis of the composition, assembly kinetics and activity of native Apaf-1 apoptosomes', *The EMBO Journal*, 23(10), pp. 2134–2145. Available at: <https://doi.org/10.1038/sj.emboj.7600210>.

Hornbeck, P.V. *et al.* (2015) 'PhosphoSitePlus, 2014: mutations, PTMs and recalibrations', *Nucleic Acids Research*, 43(D1), pp. D512–D520. Available at: <https://doi.org/10.1093/nar/gku1267>.

Hsieh, S.Y. *et al.* (2003) 'Aberrant caspase-activated DNase (CAD) transcripts in human hepatoma cells', *British Journal of Cancer*, 88(2), pp. 210–216. Available at: <https://doi.org/10.1038/sj.bjc.6600695>.

Hsu, P.P. *et al.* (2011) 'The mTOR-Regulated Phosphoproteome Reveals a Mechanism of mTORC1-Mediated Inhibition of Growth Factor Signaling', *Science*, 332(6035), pp. 1317–1322. Available at: <https://doi.org/10.1126/science.1199498>.

Iglesias-Guimaraes, V. *et al.* (2013) 'Chromatin Collapse during Caspase-dependent Apoptotic Cell Death Requires DNA Fragmentation Factor, 40-kDa Subunit-/Caspase-activated Deoxyribonuclease-

mediated 3'-OH Single-strand DNA Breaks*', *Journal of Biological Chemistry*, 288(13), pp. 9200–9215. Available at: <https://doi.org/10.1074/jbc.M112.411371>.

Inohara, N. *et al.* (1998) 'CIDE, a novel family of cell death activators with homology to the 45 kDa subunit of the DNA fragmentation factor', *The EMBO Journal*, 17(9), pp. 2526–2533. Available at: <https://doi.org/10.1093/emboj/17.9.2526>.

Inohara, N. *et al.* (1999) 'Identification of Regulatory and Catalytic Domains in the Apoptosis Nuclease DFF40/CAD *', *Journal of Biological Chemistry*, 274(1), pp. 270–274. Available at: <https://doi.org/10.1074/jbc.274.1.270>.

Ishizaki, Y., Jacobson, M.D. and Raff, M.C. (1998) 'A Role for Caspases in Lens Fiber Differentiation', *Journal of Cell Biology*, 140(1), pp. 153–158. Available at: <https://doi.org/10.1083/jcb.140.1.153>.

Kawane, K. *et al.* (1999) 'Structure and promoter analysis of murine CAD and ICAD genes', *Cell Death & Differentiation*, 6(8), pp. 745–752. Available at: <https://doi.org/10.1038/sj.cdd.4400547>.

Kerr, J.F.R., Wyllie, A.H. and Currie, A.R. (1972) 'Apoptosis: A Basic Biological Phenomenon with Wideranging Implications in Tissue Kinetics', *British Journal of Cancer*, 26(4), pp. 239–257. Available at: <https://doi.org/10.1038/bjc.1972.33>.

Kutscher, D. *et al.* (2012) 'Identification of ICAD-derived peptides capable of inhibiting caspase-activated DNase', *The FEBS Journal*, 279(16), pp. 2917–2928. Available at: <https://doi.org/10.1111/j.1742-4658.2012.08673.x>.

Larsen, B.D. *et al.* (2010) 'Caspase 3/caspase-activated DNase promote cell differentiation by inducing DNA strand breaks', *Proceedings of the National Academy of Sciences*, 107(9), pp. 4230–4235. Available at: <https://doi.org/10.1073/pnas.0913089107>.

Larsen, B.D. *et al.* (2022) 'Cancer cells use self-inflicted DNA breaks to evade growth limits imposed by genotoxic stress', *Science*, 376(6592), pp. 476–483. Available at: <https://doi.org/10.1126/science.abi6378>.

Leek, J.P. *et al.* (1997) 'Assignment of the DNA fragmentation factor gene (DFFA) to human chromosome bands 1p36.3→p36.2 by in situ hybridization', *Cytogenetics and Cell Genetics*, 79(3–4), pp. 212–213. Available at: <https://doi.org/10.1159/000134725>.

Li, P. *et al.* (1997) 'Cytochrome c and dATP-Dependent Formation of Apaf-1/Caspase-9 Complex Initiates an Apoptotic Protease Cascade', *Cell*, 91(4), pp. 479–489. Available at: [https://doi.org/10.1016/S0092-8674\(00\)80434-1](https://doi.org/10.1016/S0092-8674(00)80434-1).

Li, X., Wang, J. and Manley, J.L. (2005) 'Loss of splicing factor ASF/SF2 induces G2 cell cycle arrest and apoptosis, but inhibits internucleosomal DNA fragmentation', *Genes & Development*, 19(22), pp. 2705–2714. Available at: <https://doi.org/10.1101/gad.1359305>.

Liang, L. *et al.* (2003) 'Molecular cloning and characterization of CIDE-3, a novel member of the cell-death-inducing DNA-fragmentation-factor (DFF45)-like effector family', *Biochemical Journal*, 370(1), pp. 195–203. Available at: <https://doi.org/10.1042/bj20020656>.

Liu, X. *et al.* (1997) 'DFF, a Heterodimeric Protein That Functions Downstream of Caspase-3 to Trigger DNA Fragmentation during Apoptosis', *Cell*, 89(2), pp. 175–184. Available at: [https://doi.org/10.1016/S0092-8674\(00\)80197-X](https://doi.org/10.1016/S0092-8674(00)80197-X).

- McCarty, J.S., Toh, S.Y. and Li, P. (1999) 'Multiple Domains of DFF45 Bind Synergistically to DFF40: Roles of Caspase Cleavage and Sequestration of Activator Domain of DFF40', *Biochemical and Biophysical Research Communications*, 264(1), pp. 181–185. Available at: <https://doi.org/10.1006/bbrc.1999.1498>.
- Miura, M. *et al.* (2004) 'A crucial role of caspase-3 in osteogenic differentiation of bone marrow stromal stem cells', *The Journal of Clinical Investigation*, 114(12), pp. 1704–1713. Available at: <https://doi.org/10.1172/JCI20427>.
- Mukae, N. *et al.* (1998) 'Molecular cloning and characterization of human caspase-activated DNase', *Proceedings of the National Academy of Sciences*, 95(16), pp. 9123–9128. Available at: <https://doi.org/10.1073/pnas.95.16.9123>.
- Nagata, S. (2000) 'Apoptotic DNA Fragmentation', *Experimental Cell Research*, 256(1), pp. 12–18. Available at: <https://doi.org/10.1006/excr.2000.4834>.
- Neimanis, S. *et al.* (2007) 'Sequence Elements in Both Subunits of the DNA Fragmentation Factor Are Essential for Its Nuclear Transport*', *Journal of Biological Chemistry*, 282(49), pp. 35821–35830. Available at: <https://doi.org/10.1074/jbc.M703110200>.
- Opferman, J.T. (2008) 'Apoptosis in the development of the immune system', *Cell Death & Differentiation*, 15(2), pp. 234–242. Available at: <https://doi.org/10.1038/sj.cdd.4402182>.
- Otomo, T. *et al.* (2000) 'Structure of the heterodimeric complex between CAD domains of CAD and ICAD', *Nature Structural Biology*, 7(8), pp. 658–662. Available at: <https://doi.org/10.1038/77957>.
- Park, H.H. (2015) 'Structural insight into CIDE domains: the Janus face of CIDEs', *Apoptosis*, 20(2), pp. 240–249. Available at: <https://doi.org/10.1007/s10495-014-1067-z>.
- Sakahira, H., Enari, M. and Nagata, S. (1998) 'Cleavage of CAD inhibitor in CAD activation and DNA degradation during apoptosis', *Nature*, 391(6662), pp. 96–99. Available at: <https://doi.org/10.1038/34214>.
- Sakahira, H. and Nagata, S. (2002) 'Co-translational Folding of Caspase-activated DNase with Hsp70, Hsp40, and Inhibitor of Caspase-activated DNase*', *Journal of Biological Chemistry*, 277(5), pp. 3364–3370. Available at: <https://doi.org/10.1074/jbc.M110071200>.
- Samejima, K. and Earnshaw, W.C. (1998) 'ICAD/DFF Regulator of Apoptotic Nuclease Is Nuclear', *Experimental Cell Research*, 243(2), pp. 453–459. Available at: <https://doi.org/10.1006/excr.1998.4212>.
- Samejima, K. and Earnshaw, W.C. (2000) 'Differential Localization of ICAD-L and ICAD-S in Cells Due to Removal of a C-Terminal NLS from ICAD-L by Alternative Splicing', *Experimental Cell Research*, 255(2), pp. 314–320. Available at: <https://doi.org/10.1006/excr.2000.4801>.
- Sánchez-Osuna, M. *et al.* (2016) 'An intrinsic DFF40/CAD endonuclease deficiency impairs oligonucleosomal DNA hydrolysis during caspase-dependent cell death: a common trait in human glioblastoma cells', *Neuro-Oncology*, 18(7), pp. 950–961. Available at: <https://doi.org/10.1093/neuonc/nov315>.
- Scholz, S.R. *et al.* (2002) 'The effect of ICAD-S on the formation and intracellular distribution of a nucleolytically active caspase-activated DNase', *Nucleic Acids Research*, 30(14), pp. 3045–3051. Available at: <https://doi.org/10.1093/nar/gkf431>.

- Sievers, F. *et al.* (2011) 'Fast, scalable generation of high-quality protein multiple sequence alignments using Clustal Omega', *Molecular Systems Biology*, 7(1), p. 539. Available at: <https://doi.org/10.1038/msb.2011.75>.
- Skalka, M., Matyašová, J. and Čejková, M. (1976) 'DNA in chromatin of irradiated lymphoid tissues degrades in vivo into regular fragments', *FEBS Letters*, 72(2), pp. 271–274. Available at: [https://doi.org/10.1016/0014-5793\(76\)80984-2](https://doi.org/10.1016/0014-5793(76)80984-2).
- Song, J.H. *et al.* (2011) 'The BH3 Mimetic ABT-737 Induces Cancer Cell Senescence', *Cancer Research*, 71(2), pp. 506–515. Available at: <https://doi.org/10.1158/0008-5472.CAN-10-1977>.
- Steller, H. (1998) 'Artificial death switches: Induction of apoptosis by chemically induced caspase multimerization', *Proceedings of the National Academy of Sciences*, 95(10), pp. 5421–5422. Available at: <https://doi.org/10.1073/pnas.95.10.5421>.
- Sugimoto, N. *et al.* (1999) 'The human caspase-activated DNase gene (hCAD): genomic structure, exonic single-nucleotide polymorphisms, and a highly polymorphic dinucleotide repeat at the hCAD locus', *Journal of Human Genetics*, 44(6), pp. 408–411. Available at: <https://doi.org/10.1007/s100380050188>.
- Traven, A. and Heierhorst, J. (2005) 'SQ/TQ cluster domains: concentrated ATM/ATR kinase phosphorylation site regions in DNA-damage-response proteins', *BioEssays*, 27(4), pp. 397–407. Available at: <https://doi.org/10.1002/bies.20204>.
- Villa-Medina, M.C. *et al.* (2025) 'Cloning and Recombinant Expression of the Caspase-Activated DNase Orthologous Gene of *Giardia lamblia*', *BioMed Research International*, 2025(1), p. 3420875. Available at: <https://doi.org/10.1155/bmri/3420875>.
- Walker, J.M. (ed.) (2005) *The Proteomics Protocols Handbook*. Totowa, NJ: Humana Press. Available at: <https://doi.org/10.1385/1592598900>.
- Weil, M., Raff, M.C. and Braga, V.M.M. (1999) 'Caspase activation in the terminal differentiation of human epidermal keratinocytes', *Current Biology*, 9(7), pp. 361–365. Available at: [https://doi.org/10.1016/S0960-9822\(99\)80162-6](https://doi.org/10.1016/S0960-9822(99)80162-6).
- Widlak, P. *et al.* (2000) 'Cleavage Preferences of the Apoptotic Endonuclease DFF40 (Caspase-activated DNase or Nuclease) on Naked DNA and Chromatin Substrates*', *Journal of Biological Chemistry*, 275(11), pp. 8226–8232. Available at: <https://doi.org/10.1074/jbc.275.11.8226>.
- Widlak, P. and Garrard, W.T. (2001) 'Ionic and cofactor requirements for the activity of the apoptotic endonuclease DFF40/CAD', *Molecular and Cellular Biochemistry*, 218(1), pp. 125–130. Available at: <https://doi.org/10.1023/A:1007231822086>.
- Wiens, M. *et al.* (2003) 'Caspase-mediated apoptosis in sponges: cloning and function of the phylogenetic oldest apoptotic proteases from Metazoa', *Biochimica et Biophysica Acta (BBA) - Molecular Cell Research*, 1593(2), pp. 179–189. Available at: [https://doi.org/10.1016/S0167-4889\(02\)00388-9](https://doi.org/10.1016/S0167-4889(02)00388-9).
- Wolf, B.B. *et al.* (1999) 'Caspase-3 Is the Primary Activator of Apoptotic DNA Fragmentation via DNA Fragmentation Factor-45/Inhibitor of Caspase-activated DNase Inactivation*', *Journal of Biological Chemistry*, 274(43), pp. 30651–30656. Available at: <https://doi.org/10.1074/jbc.274.43.30651>.

Woo, E.-J. *et al.* (2004) 'Structural Mechanism for Inactivation and Activation of CAD/DFF40 in the Apoptotic Pathway', *Molecular Cell*, 14(4), pp. 531–539. Available at: [https://doi.org/10.1016/S1097-2765\(04\)00258-8](https://doi.org/10.1016/S1097-2765(04)00258-8).

Wu, C. *et al.* (2008) 'Molecular evolution of Cide family proteins: Novel domain formation in early vertebrates and the subsequent divergence', *BMC Evolutionary Biology*, 8(1), p. 159. Available at: <https://doi.org/10.1186/1471-2148-8-159>.

Wu, C.-C., Lin, J.L.J. and Yuan, H.S. (2020) 'Structures, Mechanisms, and Functions of His-Me Finger Nucleases', *Trends in Biochemical Sciences*, 45(11), pp. 935–946. Available at: <https://doi.org/10.1016/j.tibs.2020.07.002>.

Wyllie, A. (1998) 'An endonuclease at last', *Nature*, 391(6662), pp. 20–21. Available at: <https://doi.org/10.1038/34040>.

Yuste, V.J. *et al.* (2005) 'The Contribution of Apoptosis-inducing Factor, Caspase-activated DNase, and Inhibitor of Caspase-activated DNase to the Nuclear Phenotype and DNA Degradation during Apoptosis*', *Journal of Biological Chemistry*, 280(42), pp. 35670–35683. Available at: <https://doi.org/10.1074/jbc.M504015200>.

Zermati, Y. *et al.* (2001) 'Caspase Activation Is Required for Terminal Erythroid Differentiation', *Journal of Experimental Medicine*, 193(2), pp. 247–254. Available at: <https://doi.org/10.1084/jem.193.2.247>.

Zhang, J. *et al.* (1998) 'Resistance to DNA fragmentation and chromatin condensation in mice lacking the DNA fragmentation factor 45', *Proceedings of the National Academy of Sciences*, 95(21), pp. 12480–12485. Available at: <https://doi.org/10.1073/pnas.95.21.12480>.

Zhou, P. *et al.* (2001) 'Solution structure of DFF40 and DFF45 N-terminal domain complex and mutual chaperone activity of DFF40 and DFF45', *Proceedings of the National Academy of Sciences*, 98(11), pp. 6051–6055. Available at: <https://doi.org/10.1073/pnas.111145098>.